Polymer Journal, Vol. 19, No. 6, pp 757—768 (1987)

# Fiber Formation from Liquid Crystalline Precursors I. Poly(*p*-benzamide)†

G. CONIO,* R. BRUZZONE, A. CIFERRI, E. BIANCHI, and A. TEALDI*

*Istituto Chimica Industriale, Università di Genova, Corso Europa 30, 16132 Genova, Italy*

(Received August 11, 1986)

ABSTRACT: We report a study of fiber formation from solutions of poly(*p*-benzamide) (PBA) in *N*,*N*-dimethylacetamide (DMAc) containing 3% LiCl. Polymers were prepared by the Yamazaki reaction and had intrinsic viscosity between 1.37 and 1.85 dl g$^{-1}$. We analyze in detail the role of polymer concentration ($C_p$), extrusion and take-up speed, and processing temperature. Fiber properties are modest when $C_p$ is considerably below the critical concentration $C_p'$ at which the mesophase first appears. However, they improve in the pretransitional zone and exhibit a definite jump at $C_p \cong C_p'$, but tend to worsen again at $C_p > C_p'$. The velocity of the freely extruded filament, $V_f$, is smaller than the extrusion velocity $V_0$ revealing relaxation effects. There is however an optimal temperature at which $V_f/V_0 = 1$. The occurrence of these relaxation effects, and of crystallization at $C_p$ only slightly greater than $C_p'$, prevents the development of elastic moduli in excess of 50 GPa or strength above 1 GPa. Conditions for fully exploiting the orientability of the mesophase are discussed.

KEY WORDS Poly(*p*-benzamide) / Poly(*p*-phenylene terephthalamide) / Liquid Crystals / Fibers / Spinning /

Twenty years have elapsed since Kwolek[1] first reported the fiber formation from anisotropic solutions of poly(*p*-benzamide) (PBA). Although a number of more recent patents and papers have cast additional light on the spinning of nematic solutions, a critical description of the role of the several parameters involved has not been published. The lack of such a description has had a negative effect on the understanding of the revolutionary process involved. For instance, in a 1980 report Weyland[2] concluded that the mesophase is of limited or no utility in achieving ultra-high modulus and strength, a conclusion which is certainly incorrect in view of the recent advances on the technology of both lyotropic and thermotropic polymers.[3,4] One of the major point at issue is that there may not be a "jump" on the properties of *as-spun* fibers as one crosses the critical concentration at which the mesophase appears. Indeed, as it will be more fully discussed in this paper, spinning from an anisotropic dope yields ultra-high modulus fibers provided the conditions for fully exploiting the orientability of the mesophase are well understood and executed.

The earlier reports by Bair and Morgan,[5] dealing with poly(*p*-phenylene terephthalamide) (PPTA), and by Kwolek[1] do not really describe the conditions for fully exploiting the advantages of spinning from a mesophase. Indeed, the discovery of such conditions first appears in the Blades patents dealing with PPTA.[6] The discovery led to the set of properties specific of "Kevlar". These

* *Centro Macromolecule C.N.R.*

† Thesis submitted by R. Bruzzone for the Doctoral Degree in Chemistry.

conditions include the use of concentrated (99.8%) $H_2SO_4$, polymer concentration ($C_p$) ~ 20%, extrusion temperature above 80°C, an air gap.

The scientific basis for the conditions which maximize orientation and properties has not received proper elucidation. It touches on a number of fundamental problems concerning the solubility and the rheology of nematic polymers. In this paper we present new data for PBA spun from isotropic and anisotropic solutions in *N*,*N*-dimethylacetamide (DMAc)+3% LiCl. Our emphasis is on the occurrence of a "jump" on properties across the phase transition, and on the complication due to the fact that often crystallization sets in before the fluid mesophase is fully developed or completely oriented. Evidence for the latter point will be provided here, but it is already implicit in the published data collected in Figure 1. The latter represents a superimposition of rheological[7] and phase equilibria[8] results for PBA in DMAc+3% LiCl. The viscosity *vs.* concentration behavior extrapolated to zero shear stress exhibits a maximum and a minimum. At high shear stresses (close to those prevailing at the spinnerette) these singularities are suppressed and, as shown by the more extensive data of Kiss and Porter[9] for poly(γ-benzyl L-glutamate), $\eta$ increases continuously with $C_p$. The critical concentration $C'_p$ and its conjugate $C''_p$, obtained by plots of the volume fraction of isotropic phase *vs.* $C_p$[8], as well as the solubility limit ($C_p^{cryst}$) for the quiescent solution,[7] are indicated in Figure 1. These data show that: (i) the mesophase appears at a lower $C_p$ than that corresponding to the maximum (the occurrence of a shoulder and of a maximum is theoretically justified[10]), (ii) the useful concentration range between $C'_p$ and the solubility limit ($C_p^{cryst}$) is extremely small, and crystallization is responsible for the increase of $\eta$ with $C_p$ past the minimum. At high shear stress, the encroachment of crystallization to mesophase formation will be even more pronounced than indicated by the equilibrium behavior, as suggested by the disappearance of the singularity points.

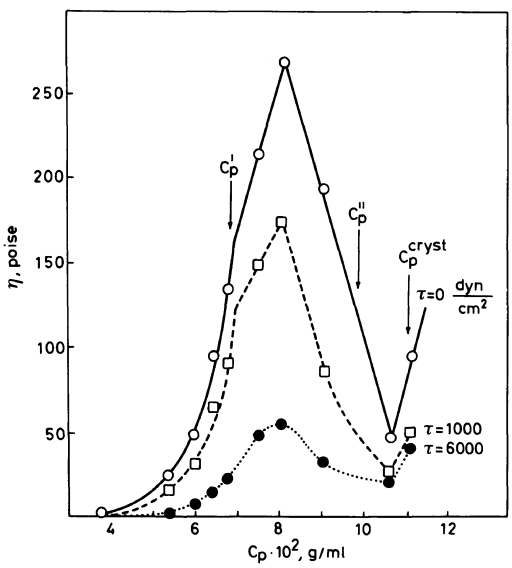


**Figure 1.** Steady state viscosity *vs.* polymer concentration for PBA in DMAc+3% LiCl at given shear stress τ. The critical concentration $C'_p$, its conjugated $C''_p$, and the solubility limit at zero stress are indicated. Data from ref 7 and 8.

## EXPERIMENTAL

### *Materials and Solutions*

Two samples of PBA (A and B) were prepared from *p*-amino benzoic acid following the method of Yamazaki *et al.*[11] Sample A ($[\eta]=1.37\,dl\,g^{-1}$) was polymerized at $T\simeq$ 110°C with a polymerization time $t$ of about 3 h. Sample B ($[\eta]=1.85\,dl\,g^{-1}$) was synthesized using $T\simeq 80$°C and $t=6$ h. Both samples were purified by dissolution in DMAc–3% LiCl followed by centrifugation at 44000 rpm for 40 hours, and precipitation of the supernatant with $H_2O$. The polymer was washed with $H_2O$ and dried under vacuum at 40°C. The intrinsic viscosity was not altered as a result of the purification procedure. Polymer concentration ($C_p$) is given as g PBA per 100 g of solution while LiCl concentration is g LiCl per dl of DMAc. Analitical grade DMAc

(BDH) and LiCl were used.

The molecular weight was determined from intrinsic viscosity in 96% $H_2SO_4$ at 25°C using the relationship[12] (valid up to $\bar{M}_w \sim 12000$)

$$[\eta] = 1.9 \times 10^{-7} \bar{M}_w^{1.7}$$

The critical concentration ($C_p'$) at which the anisotropic phase appears was determined, as previously described,[7,13] using optical microscopy supported by rheological measurements (the alternative method described in ref 8 gave similar results). The corresponding critical polymer volume fraction ($v_2'$) was calculated, as previously described,[7] using a partial specific volume of PBA $\bar{v} = 0.7542\,\mathrm{ml\,g^{-1}}$ and a specific volume of diluent $v_1 = 1.0356\,\mathrm{ml\,g^{-1}}$.[4] Concentrated solutions for spinning (dopes) were prepared by adding the DMAc + 3% LiCl diluent to the polymer; stirring at a low speed for about two weeks at room temperature. Prior to spinning, dopes were filtered through poly(propylene) gauze.

*Spinning*

The wet spinning line, manufactured by the School of Textiles, University of Bradford (U.K.), has been previously used.[15,16] Spinning conditions (and symbols) used in this work are the following.

Spinnerette die: 100 $\mu$m and length diameter ratio = 1 (connecting tubing had inner diameter of 1.16 mm and a length of 17 cm, piston diameter was 12.7 mm).

$V_0$, velocity of the spinning solution at the spinnerette die, varied in the range 4.5—12.9 $\mathrm{m\,min^{-1}}$ corresponding to shear rate at the spinnerette $\dot{\gamma} = 6000$—$17200\,\mathrm{s^{-1}}$. In particular

| $V_0/\mathrm{m\,min^{-1}}$ | $\dot{\gamma}/\mathrm{s^{-1}}$ |
|---|---|
| 4.5 | 6000 |
| 7.9 | 10500 |
| 11.1 | 14800 |
| 12.9 | 17200 |

$V_1$, velocity at the first set of rollers.

$V_2$, velocity at the second set of rollers.

$V_R$, velocity at the bobbin.

The $V_1/V_2$ and $V_1/V_R$ ratios were invariably kept equal to 1. Coagulation bath: $H_2O$ (occasionally $H_2O$ + 5 to 60% DMAc). $T$ of coagulation bath: varied between 20°C and 75°C. Washing bath, $H_2O$ at room temperature. Air Gap, usually not used. As-spun fibers were washed in running water for 12 hours, left in distilled water for about 24 hours, dried under vacuum at 50°C for 24 hours, and finally stored over $CaCl_2$ until testing. No post-spinning (thermal or mechanical) treatments were performed.

*Fiber Properties*

The apparent fiber diameter was determined with a Reichert Zetopan optical microscope as previously described.[15] The apparent diameter varied between 15 and 50 $\mu$m, corresponding to denier between 2 and 25 ($\mathrm{den} = \pi(d/2)^2 \times 9000 \times 1.45 \times 100$). To obtain a better picture of the cross-sectional shape, bundles of ~40 monofilaments were imbibed in an epoxy resin (Durcupan ACM). A rod of ~5 cm was obtained out of which sections of 0.1 $\mu$m were cut using a diamond knife and a Reichert $OmU_2$ microtome. Cutting was performed at room temperature, speed $2.5\,\mathrm{mm\,s^{-1}}$, orienting the rod so that the knife edge was perpendicular to the fiber axis. Sections were transferred to electron microscope grids and observed under the optical microscope (× 630) or with an electron microscope T.E.M. Siemens Elmiskop 102 (× 3000 to × 12000). It is possible, by electron diffraction, to test the existence or not of a radial orientation of crystallites (LCO) in a fiber.[6] We followed the technique of Blades,[6] but (in contrast with PPTA) PBA did not show this kind of orientation. Mechanical properties were determined using an Instron Model 1122 Tensile machine operating at room temperature[15] with an initial deformation rate of $0.1\,\mathrm{min.^{-1}}$ Elastic modulus ($E$), strength ($\sigma_b$) and elongation to break ($\varepsilon_b$) are averages on 5 independent determinations using bundles of 4 untwisted filaments. The relationship

between the GPa units (preferentially used) and g/den (density $\cong 1.45$) is 1 GPa $\sim 8.0$ g den$^{-1}$.

## RESULTS AND DISCUSSION

Sample characteristics, including the critical concentration at which the mesophase appears, are collected in Table I.

### *Fiber Cross-Sections*

Typical fiber cross-sections are illustrated in Figure 2. Considerable deviations from the circular cross-section were noticed, particularly when spinning was performed from isotropic solutions at low $C_p$. Similar effects are attributed by Ziabicki[17] to a difference between the deformability of the thin surface layer and the inner core, associated to an inward flux of non-solvent lower than the outward solvent flow. Various approaches were used to evaluate the cross-sectional area needed for the determination of the modulus. Use of the apparent diameter, $d_{app}$, observed under the microscope, and the assumption of a circular section, was satisfactory for fibers spun at large $C_p$, as suggested in Figure 2. However, due to the significant deviations illustrated in Figure 2, the use of $d_{app}$ would have cast doubts on the moduli corresponding to isotropic dopes. Therefore, we evaluated the effective cross-sectional area from the equation of mass balance

$$V_0 \cdot S_0 \cdot c_p = V_1 \cdot S_1 \cdot \rho \qquad (1)$$

where $S_0$ and $S_1$ are the cross-sectional areas (in cm$^2$) of the die and of the fiber respectively, $c_p$ is the polymer concentration in g ml$^{-1}$ and $\rho$ is the polymer density (1.45 g ml$^{-1}$). Values of $S_1$ are included in Tables II, III, and IV along with corresponding $V_0$ and $V_1$ values. Two additional attempts to evaluate a cross-sectional area which included fiber voids were made. One was the evaluation of the effective section using photographs similar to those in Figure 2. The other was based on the weight of

**Table I.** Characteristics of samples investigated

| Sample | $[\eta]$/dl g$^{-1}$ [a] | $\bar{M}_v$ | $C'_p$/%[b] | $v'_2$[b] |
|---|---|---|---|---|
| A | 1.37 | 10800 | 6.8 | 0.050 |
| B | 1.85 | 12900 | 5.7 | 0.042 |

[a] In 96% $H_2SO_4$.
[b] In DMAc + 3% LiCl.

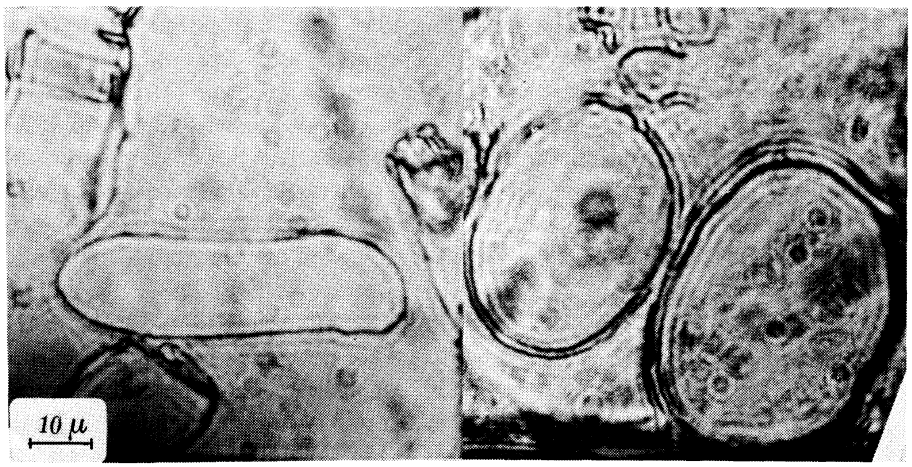


a b

**Figure 2.** Micrographs of fiber cross-sections for PBA sample B obtained when spinning at $C_p = 5.4\%$ (a) and at $C_p = 5.9\%$ (b). $V_1/V_f = 1$.

**Table II.** Fiber properties when $C_p < C'_p$[a]

| $C_p$/% w/w | $V_0$/m min$^{-1}$ | $V_1$/m min$^{-1}$ | $V_1/V_f$ | $S_1/10^5$ cm$^2$ | $E$/GPa | $\sigma_b$/GPa | $\varepsilon_b$/% |
|---|---|---|---|---|---|---|---|
| | | | Sample A ($C'_p$=6.8%) | | | | |
| 4.4 | 7.9 | 3 | 1 | 0.613 | 12.0 | 0.25 | 22.3 |
| 4.4 | 7.9 | 4.3 | 1.4 | 0.428 | 13.0 | 0.27 | 21.7 |
| 4.4 | 7.9 | 6.6 | 2.2 | 0.278 | 12.8 | 0.26 | 13.0 |
| 4.4 | 11.1 | 3.4 | 1 | 0.757 | 11.9 | 0.25 | 21.3 |
| 4.4 | 11.1 | 6.8 | 2 | 0.378 | 11.1 | 0.23 | 23.4 |
| 4.4 | 11.1 | 9.7 | 2.9 | 0.263 | 10.1 | 0.22 | 14.2 |
| 4.4 | 12.9 | 6 | 1.4 | 0.501 | 13.3 | 0.25 | 14.2 |
| 6.0 | 7.9 | 4.4 | 1 | 0.572 | 12.4 | 0.21 | 19.0 |
| 6.0 | 7.9 | 8.25 | 1.9 | 0.305 | 11.2 | 0.22 | 16.0 |
| 6.0 | 7.9 | 13.05 | 3 | 0.192 | 13.8 | 0.27 | 11.0 |
| 6.0 | 12.9 | 6.75 | 1 | 0.609 | 11.9 | 0.19 | 9.5 |
| 6.3 | 4.5 | 3.8 | 1 | 0.398 | 16.2 | 0.22 | 8.8 |
| 6.3 | 4.5 | 7.6 | 2 | 0.199 | 17.7 | 0.25 | 9.3 |
| 6.3 | 7.9 | 5 | 1 | 0.530 | 15.8 | 0.24 | 10.8 |
| | | | Sample B ($C'_p$=5.7%) | | | | |
| 3.0 | 7.9 | 4.25 | 1 | 0.292 | 16.0 | 0.33 | 7.9 |
| 4.3 | 4.5 | 3.2 | 1 | 0.320 | 16.7 | 0.33 | 9.0 |
| 4.3 | 4.5 | 6.4 | 2 | 0.160 | 17.4 | 0.40 | 9.0 |
| 4.3 | 4.5 | 9.6 | 3 | 0.107 | 18.5 | 0.56 | 7.2 |
| 4.3 | 7.9 | 4.2 | 1 | 0.428 | 14.4 | 0.31 | 15.0 |
| 4.3 | 7.9 | 8.8 | 2.1 | 0.204 | 15.5 | 0.33 | 15.0 |
| 4.3 | 7.9 | 14 | 3.3 | 0.129 | 16.5 | 0.33 | 10.0 |
| 4.3 | 12.9 | 7 | 1 | 0.419 | 17.0 | 0.28 | 13.0 |
| 5.2 | 4.5 | 2.6 | 1 | 0.476 | 16.2 | 0.38 | 11.5 |
| 5.2 | 4.5 | 7.8 | 3 | 0.159 | 29.1 | 0.50 | 7.0 |
| 5.2 | 12.9 | 7.25 | 1.1 | 0.490 | 19.9 | 0.43 | 11.8 |
| 5.2 | 12.9 | 14.3 | 2 | 0.248 | 25.4 | 0.52 | 8.2 |
| 5.4 | 4.5 | 2.8 | 1 | 0.460 | 17.2 | 0.37 | 10.5 |
| 5.4 | 4.5 | 8.4 | 3 | 0.153 | 25.8 | 0.51 | 6.3 |
| 5.4 | 7.9 | 4.7 | 1.1 | 0.482 | 24.3 | 0.43 | 8.6 |
| 5.4 | 7.9 | 14.3 | 3 | 0.158 | 32.9 | 0.58 | 5.4 |
| 5.4 | 12.9 | 7.6 | 1.2 | 0.486 | 20.6 | 0.46 | 9.9 |
| 5.4 | 12.9 | 14.4 | 2 | 0.257 | 28.4 | 0.53 | 8.1 |

[a] $T_{bath}$=20°C.

a given length of fiber and its actual density. These two approaches applied to sample A ($C_p$=6.0 and 7.1%) and sample B ($C_p$=5.9%) gave areas within ±10% from the $S_1$ value in Table III. Unfortunately, the large experimental indetermination prevents any conclusions concerning fiber voids.

*Die Swell*

Figure 3 illustrates the relationship between $V_f$ and $V_0$ at 20°C. The ratio $V_f/V_0$ decreases from 1 to ~0.6 when $V_0$ is increased. Moreover, $V_f/V_0$ slightly decreases with decreasing concentration. Additional data reported in Table IV indicate that $V_f/V_0$ increases with temperature, attains the value ~1 at ~50°C, and decreases again upon further increase of temperature.

The pull off ratio during coagulation is given below as $V_1/V_f$. It was calculated using Figure 3 for any given $V_0$.

Equation 1, applied to the only case in

which $V_0 = V_f = V_1$ (Table IV, $T = 55°C$), yields the minimum value of the fiber cross-section, $S_{1,min}$, under conditions of no pull-off ($V_1/V_f = 1$). Under the more common cases for which $V_0 > V_f$, and still no pull-off ($V_1/V_f = 1$), $S_1 > S_{1,min}$. The square-root of the $S_1/S_{1,min}$ ratio calculated using the data in Tables II and III is usually in the range 1.10 to 1.40, the lower values occurring in the anisotropic solutions. We tentatively interpret this observation as evidence of die swelling due to the elasticity of the spinning dope. When data at constant $V_1/V_f$ are considered, an increase of die swell is reflected in fibers with reduced orientation. Die swelling for rigid polymers and anisotropic solutions is somewhat unexpected since relaxation times for nematic domains should be rather large.[18,19] Nevertheless, die swelling has been evidenced by Celanese investigators[20] for PPTA (air gap) using photographic techniques.

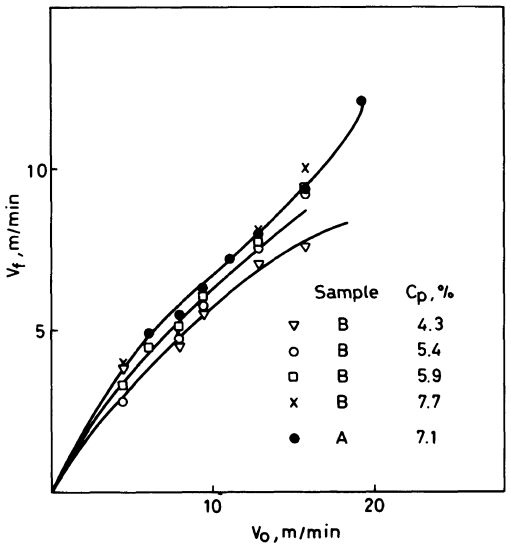


**Figure 3.** Variation of the free velocity ($V_f$) with extrusion rate for PBA solutions of samples A or B having different polymer concentration. $T_{bath} = 20°C$.

The postulated relaxation mechanisms responsible for the slowing down of the filament at the die exit would appear to decrease when $V_0$ (or $\dot{\gamma}$) is decreased, $C_p$ is increased, and the temperature is increased up to $\sim 50°C$. It is surprising that $V_f/V_0$ decreases again at still higher temperatures. Ziabicki[17] suggested that die swelling is maximum when the coagulation

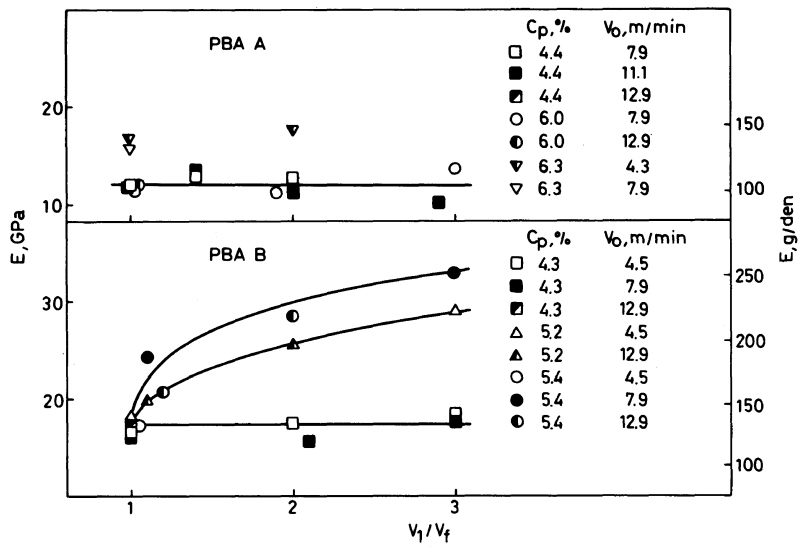


**Figure 4.** Modulus of fibers of PBA (sample A above, sample B below) spun from isotropic solutions *vs.* pull off ratio. Temperature of coagulation bath is 20°C. Values of dope concentration and extrusion rate are indicated.

is retarded, an effect expected at higher temperature. On the other hand, the friction between the filament and the coagulating bath could enhance the tendency of the filament to die swell. The friction is controlled by the viscosity of water which is considerably reduced between 20° and 50°C. A competition between the latter effects could be advocated to explain the minimum die swell at ~50°C.

*Fiber Properties when* $C_p < C'_p$

Figure 4 and Table II illustrate the effect of pull off ratio $V_1/V_f$ on the properties of fibers of samples A and B spun from isotropic dopes. Data are representative of several values of extrusion rate $V_0$ and concentration $C_p$. In all cases, however, $C_p < C'_p$ ($C'_p = 6.8$ and 5.7, respectively, for samples A and B). The modulus (plotted in Figure 4) appears relatively small (10—18 GPa) and is not affected by concentration when the dope is definitively isotropic ($C_p$ considerably smaller than $C'_p$). Neither the pull off ratio nor the extrusion rate have an effect. Only in the pretransitional region close to $C'_p$ (see particularly $C_p = 5.2$ and 5.4% for sample B) does the modulus begin to increase with $V_1/V_f$, reaching values of $E \sim 30$ GPa for sample B. These values of pretransitional modulus are already within the ultra-high modulus range. Larger values will be attained only if we enter the transition region centered at $C'_p$.

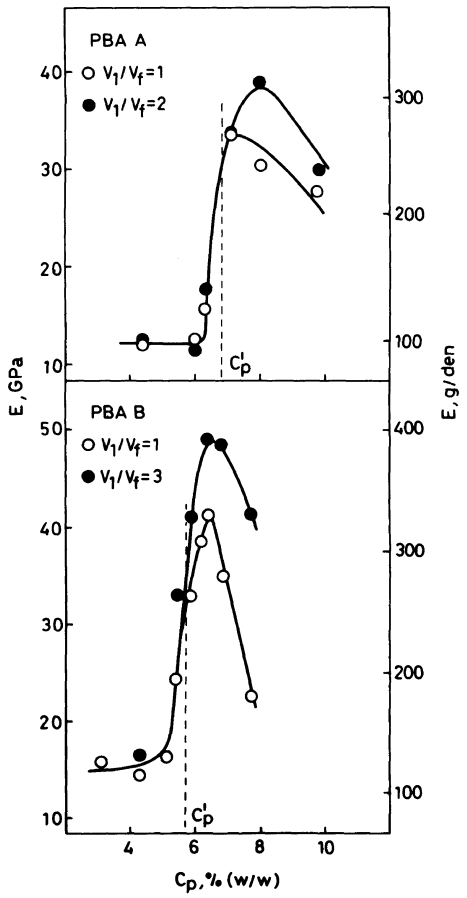


**Figure 5.** Modulus of as-spun fibers of PBA (sample A above, sample B below) *vs.* polymer concentration extending into the anisotropic region. Values of pull off ratio are indicated. $V_0 = 7.9$ m min$^{-1}$. $T_{bath} = 20$°C. Dotted lines indicate $C'_p$.

*Fiber Properties when* $C_p \cong C'_p$

Figure 5 and Table III illustrate the effect of concentration on the properties in the $C_p$ range which includes the critical value. Data are for both samples A and B, and include the effect of pull off ratio.

In the case of sample A the modulus (plotted in Figure 5) jumps from 15.7 GPa at $C_p = 6.3\%$ to 33.6 GPa at $C_p = 7.1\%$ ($C'_p$ is 6.8%). Up to this concentration level the modulus is not affected by $V_1/V_f$. However, upon further increasing $C_p$ the modulus decreases if $V_1/V_f = 1$, but continues to increase if $V_1/V_f = 2$.

Similar, but more pronounced effects are shown by sample B which has a larger molecular weight, and lower $C'_p$ ($= 5.7\%$), than sample A. The pull off ratio is effective in increasing the modulus already in the pretransitional range ($C_p > 5.2\%$). When $V_1/V_f = 1$ the modulus jumps from 16.2 GPa at $C_p = 5.2\%$ to 33.1 GPa at $C_p = 5.9\%$. When $V_1/V_f = 3$ the modulus attains 41.0 GPa at $C_p = 5.9\%$. These dramatic effects, centered at $C'_p$, leave no doubt that ultra-high modulus is directly connected with the appearance of the mesophase.

Weyland,[2] working with PPTA/$H_2SO_4$ at 40°C, failed to observe a jump of the modulus at $C'_p$. However $C'_p$ was improperly deduced from the maximum (rather than the shoulder) on the $\eta$ *vs.* $C_p$ plot, as discussed elsewhere.[18] We should also point out that the use of eq 1 for assessing the cross-sectional areas produced moduli in the isotropic region (10—18 GPa, or 80—150 g den$^{-1}$) which tend to be larger (by a factor of up to 2) than those reported by others.[1,2,16] Had we used $d_{app}$ to calculate the cross-section, the latter moduli would have been considerably reduced (no much effect being evident for the moduli in the anisotropic region), making even more pronounced the jump of properties across the transition.

*Fiber Properties when* $C_p > C'_p$

Inspection of Figure 5 and Table III reveals that further increase of $C_p$ above 5.9% for sample B, causes an additional increase of modulus which is however not as pronounced as that observed within the transition region. There is definitively a tendency to a decrease of modulus when $C_p$ is significantly larger than $C'_p$. For instance, for sample B at $C_p = 6.4\%$ the modulus reaches a maximum of 41.3 and 48.9 GPa, respectively for $V_1/V_f = 1$ and $V_1/V_f = 3$. Eventually the modulus starts to diminish and at $C_p = 7.7\%$ has decreased to 22.4 and 41.3 GPa, respectively for $V_1/V_f = 1$ and $V_1/V_f = 3$. Similar effects were observed by Weyland[2] working with PPTA in $H_2SO_4$ at 40°C (*cf.* seq.). These results suggest that as soon as the mesophase in encountered improved fluid orientability leads to ultra-high modulus. However, almost simultaneously a complication occurs which prevents the full exploitation of the mesophase for obtaining still larger values of orientation and modulus. This complication, as discussed in the introductory section, is the earlier occurrence of crystallization along the spinline. Moreover, the fluid at the exit from the die loses some orientation which tends to be reestablished by a $V_1/V_f > 1$. However, at the same time, crystallization begins in the coagulation bath. Therefore, in order to maximize properties it is essential that the mesophase is fully developed and oriented before crystallization sets in.

The effect of extrusion rate on the modulus when $C_p > C'_p$ is shown in Figure 6 for sample B ($C_p = 7.7\%$). It is seen that the modulus

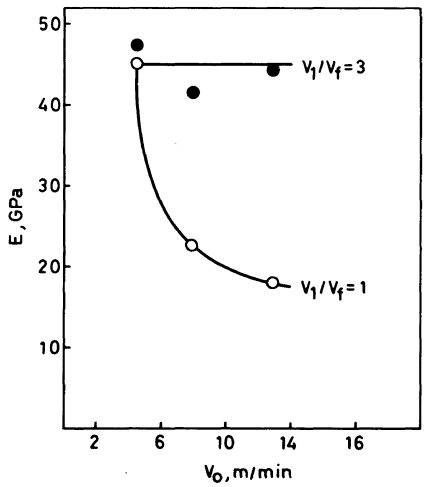


**Figure 6.** Modulus of as-spun fiber of PBA sample B *vs.* extrusion rate for the indicated value of pull off ratio. $C_p = 7.7\%$. $T_{bath} = 20°C$.

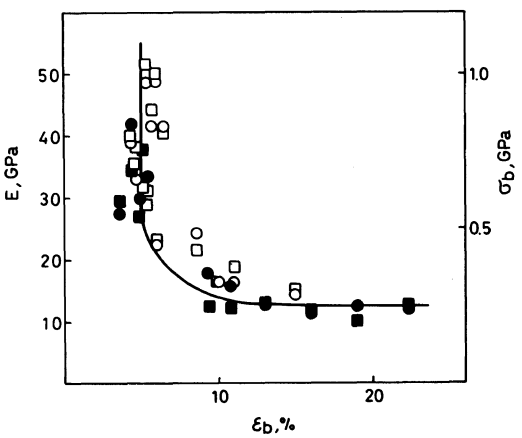


**Figure 7.** Modulus (○), tensile strength (□) and elongation to break for PBA sample A (full points) and B (open points). Data from Table III cover several $C_p$ and $V_1/V_f$ values. $T_{bath} = 20°C$, $V_0 = 7.9$ m min$^{-1}$.

**Table III.** Fiber properties[a]

| $C_p$/% w/w | $V_f$/m min$^{-1}$ | $V_1/V_f=1$ | | | | $V_1/V_f\simeq 2$ | | | |
|---|---|---|---|---|---|---|---|---|---|
| | | $S_1/10^5$ cm$^2$ | $E$/GPa | $\sigma_b$/GPa | $\varepsilon_b$/% | $S_1/10^5$ cm$^2$ | $E$/GPa | $\sigma_b$/GPa | $\varepsilon_b$/% |
| | | | | | Sample A ($C_p'=6.8\%$) | | | | |
| 4.4 | 3.0 | 0.613 | 12.0 | 0.25 | 22.3 | 0.278 | 12.8 | 0.26 | 13.0 |
| 6.0 | 4.4 | 0.573 | 12.4 | 0.21 | 19.0 | 0.305 | 11.2 | 0.22 | 16.0 |
| 6.3 | 5.0 | 0.530 | 15.7 | 0.24 | 10.8 | 0.260 | 17.7 | 0.25 | 9.3 |
| 7.1 | 5.5 | 0.475 | 33.6 | 0.61 | 5.5 | 0.230 | 33.4 | 0.63 | 5.3 |
| 8.0 | 4.6 | 0.735 | 30.3 | 0.38 | 5.2 | 0.352 | 39.0 | 0.69 | 4.4 |
| 9.8 | 5.4 | 0.760 | 27.6 | 0.53 | 3.6 | 0.385 | 29.8 | 0.52 | 5.9 |
| | | | | | Sample B ($C_p'=5.7\%$) | | | | |
| | | $V_1/V_f=1$ | | | | $V_1/V_f\simeq 3$ | | | |
| 4.3 | 4.2 | 0.428 | 14.4 | 0.31 | 15.0 | 0.129 | 16.5 | 0.33 | 10.0 |
| 5.2 | 4.6 | 0.466 | 16.2 | 0.38 | 11.0 | — | — | — | — |
| 5.4 | 4.7 | 0.482 | 24.3 | 0.43 | 8.6 | 0.158 | 32.9 | 0.58 | 5.4 |
| 5.9 | 5.1 | 0.487 | 33.1 | 0.68 | 5.7 | 0.171 | 41.0 | 0.86 | 5.3 |
| 6.2 | 4.9 | 0.526 | 38.6 | 0.72 | 5.5 | — | — | — | — |
| 6.4 | 5.2 | 0.512 | 41.3 | 0.82 | 6.5 | 0.185 | 48.9 | 1.00 | 6.0 |
| 6.8 | 4.9 | 0.590 | 35.0 | 0.70 | 4.3 | 0.199 | 48.6 | 1.03 | 5.3 |
| 7.7 | 5.1 | 0.637 | 22.4 | 0.47 | 6.0 | 0.205 | 41.3 | 0.88 | 5.7 |

[a] $T_{bath}=20°C$; $V_0=7.9$ m min$^{-1}$.

decreases with increasing extrusion rate when $V_1/V_f=1$, and remains essentially unchanged when $V_1/V_f=3$. $\sigma_b$ (unreported) follows a similar trend. These effects are a clear manifestation of the competition between fluid relaxation at the die (increasing with $V_0$, *cf.* Figure 3) and spinline tension.

Strength and elongation to break data from Table III for $V_0=7.9$ m min$^{-1}$ are plotted in Figure 7. The trend of the curve defined by this plot is similar to that previously reported.[16] Although the individual concentrations are not labeled in the graph, data for $C_p<C_p'$ fall along the right hand horizontal portion of the curve. The sharp upturn of the curve reflects the improvement of all mechanical properties resulting from the transition.

Comparison of the data obtained for samples A and B (Table III) reveals that an increase of molecular weight improves both $E$ and $\sigma_b$. A particularly beneficial effect on $\sigma_b$ is expected at still larger values of $\bar{M}_t$ than those employed here. The strength exhibited by our fibers (maximum was 1 GPa) is somewhat below that reported in the patent literature due to the low molecular weight and the limitation of our spinning conditions. The denier of our fibers is instead comparable with values in the patent literature.

*Maximizing Properties*

Properties can be improved by post-spinning treatments (not considered here) or, at as-spun level, by operating on such variables as extrusion and coagulation temperature, air gap, solvent/non solvent system, $C_p$, $V_0$, $V_1$ and polymer molecular weight. The effect of the last four mentioned parameters is described by the data already presented. The guideline for maximizing properties is the achievement of conditions under which crystallization sets is when mesophase orientation is well developed.

We have attempted the use of an air gap[6,21] between the die and the coagulation bath. The air gap is expected to have a beneficial effect

due to the occurrence of a region where elongational flow occurs, while the increase of $C_p$ which occurs in the coagulation bath is delayed. We were able to apply an air gap of $\sim 2$ cm only to sample B (drop formation was observed for sample A). A fiber obtained from a dope with $C_p = 5.9\%$, $V_1/V_f = 1$, $V_0 = 7.9\,m\,min^{-1}$ exhibited a modulus of 35 GPa, only slightly larger than obtained without air gap (*cf.* Table III). It appears that an air gap has no large effect when spinning from organic solvents. By contrast, it has a large effect when PPTA is spun from $H_2SO_4$ at $C_p \sim 20\%$.[6]

Another attempt to improve properties was an alteration of the composition of the coagulation bath. By using a mixture containing up to 10% DMAc (90% $H_2O$) no significant improvement of fiber properties was obtained. Using also LiCl (DMAc 20%, LiCl 2%) the modulus started to decrease, suggesting that coagulation should not be unduly delayed.

Still another attempt consisted in an increase of the temperature of the coagulation bath up to 75°C. Because we are dealing with a conventional wet spinning process (die immersed in the coagulation bath) the temperatures of extrusion ($T_{ext}$) and of coagulation ($T_{bath}$) are nearly the same. Results for sample B ($C_p = 5.9\%$, $V_0 = 7.9\,m\,min^{-1}$) are collected in Table IV. Two values of the $V_1/V_f$ ratio were employed. Both $E$ and $\sigma_b$ remain large, but the actual values are not increased over the largest 20°C values reported in Table III.

The data in Table IV do however show the interesting effect that a maximum on $E$ and $\sigma_b$ is obtained when $T_{bath} \sim 50$°C. As already pointed out, die swell is also affected by $T_{bath} \cdot V_f/V_0$ increases to $\sim 1$ at $\sim 50$°C when the fiber section attains a minimum, and the modulus a maximum. The observation clearly support the view that better properties result when fluid orientation is not allowed to relax.

## FINAL REMARKS

The jump of mechanical properties at the critical concentration assumes particular significance when one consider that: (i) at $C_p \sim C_p'$ we are still close to the biphasic gap[22] and therefore some amount of isotropic phase may coexist with the anisotropic one[23]; (ii) there seems to be an appreciable die swelling which reduces the orientation achieved by the solution along the connecting tubing. Occurrence of crystallization for this incompletely formed, incompletely oriented mesophase already produces a respectable modulus of up to $\sim 40$ GPa. Counteracting the die swell with larger $V_1/V_f$, $C_p$, or with an optimal spinning temperature, may rise the modulus up to $\sim 50$ GPa. Correspondingly, the strength

**Table IV.** Effect of temperature of coagulation on fiber-properties (Sample B)

| $V_1/V_f$ | $T_{bath}$/°C | $V_f$/m min$^{-1}$ | $V_f/V_0$ | $S_1$ / cm$^2 \times 10^5$ | $E$/GPa | $\sigma_b$/GPa | $\varepsilon_b$/% |
|---|---|---|---|---|---|---|---|
| 1 | 20 | 5.1 | 0.64 | 0.487 | 33.1 | 0.68 | 5.7 |
| 1 | 45 | 5.7 | 0.71 | 0.435 | 37.0 | 0.72 | 8.6 |
| 1 | 55 | 8.0 | 1.0 | 0.297 | 36.0 | 0.70 | 4.2 |
| 1 | 65 | 7.6 | 0.95 | 0.324 | 34.1 | 0.64 | 7.0 |
| 1 | 75 | 6.7 | 0.84 | 0.375 | 27.4 | 0.66 | 8.1 |
| 2 | 20 | 5.1 | 0.65 | 0.243 | 38.0 | 0.78 | 5.3 |
| 2 | 40 | 5.7 | 0.72 | 0.218 | 44.6 | 0.79 | 5.3 |
| 2 | 55 | 8.0 | 1.0 | 0.168 | 40.8 | 0.75 | 5.2 |

[a] $V_0 = 7.9\,m\,min^{-1}$; $C_p = 5.9\%$.

may reach up to 1 GPa ($\sim 8\,g\,den^{-1}$). Now we should ask: how can we reach still higher figures—the theoretical ones, or these reported for Kevlar ($E \rightarrow 1000\,g\,den^{-1}$, $\sigma_b \rightarrow 20\,g\,den^{-1}$, $\varepsilon < 5\%$)?

It is relevant to analyze conditions under which rigid polymers exhibit large solubility ($C_p^{cryst} \gg C_p'$) at accessible temperatures. Formation of complexes between the polymer and solvent components *in solution* causes a large depression of the melting temperature (or "salting-in").[22] These effects may be particularly intense when binding gives rise to complexes which *crystallize* at a temperature ($T_m^*$) well below the (high) melting temperature of the pure rigid polymer ($T_m^\circ$).[25] Crystallosolvates involving PBA, DMAc and LiCl,[26] or PPTA and $H_2SO_4$,[27] have in fact been reported, although complete phase diagrams involving the corresponding solutions have not been fully elucidated.

Jingsheng *et al.*,[28] as well as Gardner *et al.*,[27] have however reported solubility data for the PPTA/$H_2SO_4$ system which allow a schematic representation of the salient features of the phase diagram. The latter is reported in Figure 8. When $C_p$ is decreased from 22 to 12%, $T_m$ decreases from $\sim 80°$ to 20°C, according to the results of the above authors (illustrated in detail in the insert). The solubility of PBA in DMAc+LiCl is preliminarily assessed to be smaller than that of PPTA in $H_2SO_4$. Hence the greater interest in the latter system. $T_m^\circ$ for both polymers is reported[26,27] in the order of 550°C. $T_m^*$ of the pure crystallosolvate is in the order of 210°C,[26,27] but the compositions are not well known.

The conditions relevant to the spinning of PPTA according to Blades[6] are indicated by a cross ($C_p = 20\%$, $T > 80°C$) in Figure 8. As pointed out by Jaffe and Jones,[20] since high dope concentration requires $T > 80°C$, the use of an air gap becomes necessary. The coagulated crystallosolvate reverts to the pure polymer when the fiber is washed.[26]

The conditions relevant to the spinning of

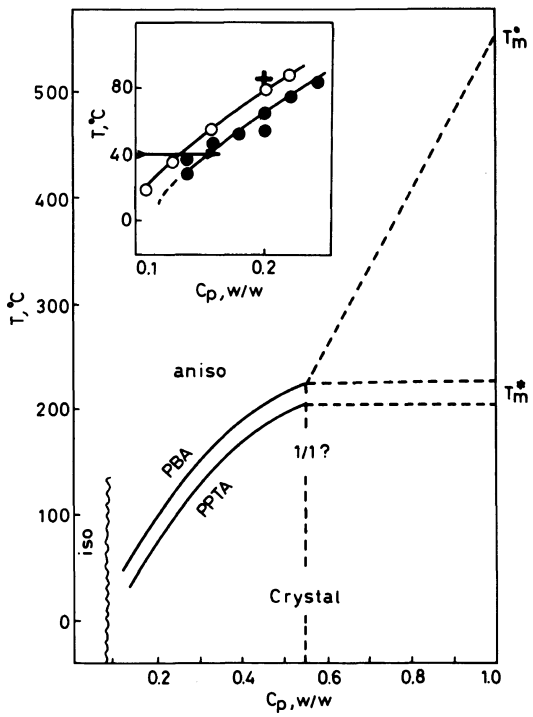


**Figure 8.** Idealized representation of the phase diagram of the PPTA/$H_2SO_4$ and PBA/DMAc+LiCl systems. In the enlarged insert, experimental points for the former polymer system are those by Jingsheng *et al.*[28] (○), and by Gardner *et al.*[27] (●). $T_m^\circ$ and $T_m^*$ data are from ref 20, 26, 27.

PPTA in $H_2SO_4$ at 40°C according to Weyland[2] are illustrated by the horizontal arrow in Figure 8. He spuns dopes with $C_p$ from 3 to 15% (no air gap), obviously crossing the crystallization boundary. Therefore, as already pointed out, he observed a decrease of modulus at $C_p > C_p'$, a fact which led him to the erroneous conclusions mentioned in the Introduction.

The large improvement in properties when $C_p$ is as high as 20% and $T > 80°C$ are not unexpected since the cross-sectional shape improves with $C_p$ and die swelling decreases with $T$ (Table IV) and $C_p$. This facilitates the retention of the domain alignment just past the die.[18] Also, the microscopic order of the liquid crystal, described by the order parameter, has been shown to increase when $C_p$ is increased.[29]

Furthermore, asymmetric attractive interactions could become relevant at large $C_p$, possibly leading to a higher degree of order than that of the uniaxial nematic[18] and perhaps explaining the lateral crystalline orientation (LCO) reported by Blades.[6]

*Acknowledgment.* Much of the results presented here might have been obvious to the investigators whose work is reported in the earlier patents.[1,6] To those investigators goes the credit of truly pioneering work. We express our appreciation to Prof. G. Marrucci for precious suggestions concerning the treatment of data, and to Mr. G. Dondero for the preparation of fiber cross-sections.

## REFERENCES

1. S. L. Kwolek, U. S. Patent 3,671,542 (1972) (to du Pont Co.), originally filed 13/6/1966.
2. H. A. Weyland, *Polym. Bull.*, **3**, 331 (1980).
3. A. Ciferri and I. M. Ward, Ed., "Ultra-High Modulus Polymers," Applied Science Publishers, London, 1979.
4. L. L. Chapoy, Ed., "Recent Advances in Liquid Crystalline Polymers," Elsevier Applied Science Publishers, Ltd., London, 1985.
5. T. I. Bair and P. W. Morgan, Br. Patent 1,259,788 (1972) (to du Pont Co.), filed in the U. S. 27/12/1967.
6. H. Blades, U. S. Patent 3,869,429 (1975) (to du Pont Co.), filed 17/8/1971.
7. C. Balbi, E. Bianchi, A. Ciferri, A. Tealdi, and W. R. Krigbaum, *J. Polym. Sci., Polym. Phys. Ed.*, **18**, 2037 (1980).
8. G. Conio, E. Bianchi, A. Ciferri, and A. Tealdi, *Macromolecules*, **14**, 1084 (1981).
9. G. Kiss and R. S. Porter, *J. Polym. Sci., Polym. Phys. Ed.*, **18**, 361 (1980).
10. R. R. Matheson, Jr., *Macromolecules*, **13**, 643 (1980).
11. N. Yamazaki, M. Matsumoto, and F. Higashi, *J. Polym. Sci., Polym. Chem. Ed.*, **13**, 1373 (1975).
12. J. R. Schaefgen, V. S. Foldi, F. M. Logullo, V. H. Good, L. W. Gulrich, and F. L. Killian, *Polym. Prepr. Am. Chem. Soc., Div. Polym. Chem.*, **17**, 69 (1976).
13. A. Ciferri, "Polymer Liquid Crystals," A. Ciferri, W. R. Krigbaum, and R. B. Mayer, Ed., Applied Science Publishers, London, 1979.
14. E. Bianchi, A. Ciferri, and A. Tealdi, *Macromolecules*, **15**, 1268 (1982).
15. B. Valenti, G. C. Alfonso, A. Ciferri, P. Giordani, and G. Marrucci, *J. Appl. Polym. Sci.*, **26**, 3643 (1981).
16. G. C. Alfonso, E. Bianchi, A. Ciferri, S. Russo, F. Salaris, and B. Valenti, *J. Polym. Sci., Polym. Symp.*, **65**, 213 (1978).
17. A. Ziabicki, "Physical Foundations of Fiber Formation," Wiley, New York, 1976.
18. A. Ciferri, "Developments in Oriented Polymers-2," I. M. Ward, Ed., Elsevier Applied Science Publishers, Ltd., 1986.
19. G. Marrucci, IUPAC Symposium on Non Crystalline Order in Polymers, Naples, Italy, May 1985; IX International Congress of Rheology, B. Mena, A. Garcia Rejon, and C. Range Naisale, Ed., University National Aut. de Mexico, Acapulco, 1984, p 441.
20. M. Jaffe and R. Sidney Jones, "High Technology, Fibers," Part A, M. Lewin and J. Preston, Ed., M. Dekker, New York, 1985, Part A, p 349.
21. *Cf. e.g.*, U. S. Patent 3,414,645 (1975) (to Monsanto Co.).
22. P. J. Flory, *Adv. Polym. Sci.*, **56**, 1 (1984).
23. G. Marrucci and A. Ciferri, *J. Polym. Sci., Polym. Lett.*, **15**, 643 (1977).
24. T. A. Orofino, A. Ciferri, and J. J. Hermans, *Biopolymers*, **5**, 773 (1967).
25. S. P. Papkov, *Adv. Polym. Sci.*, **59**, 75 (1984).
26. M. Takase, A. Ciferri, and W. R. Krigbaum, *J. Polym. Sci., Polym. Phys. Ed.*, in press.
27. K. H. Gardner, R. R. Matheson, P. Avakian, Y. T. Chia, and T. D. Gierke, "Polymers for Fibers and Elastomers," American Chemical Society, 1984.
28. B. Jingsheng, Y. Anjii, Z. Shengging, Z. Shufan, and H. Chang, *J. Appl. Polym. Sci.*, **26**, 1211 (1981).
29. M. L. Sartirana, E. Marsano, E. Bianchi, and A. Ciferri, *Macromolecules*, **19**, 1176 (1986).